Article

Not peer-reviewed version

Unveiling New Physics Models Through Meson Decays and Their Impact on Neutrino Experiments

Adriano Cherchiglia *

Posted Date: 14 May 2025

doi: 10.20944/preprints202505.1067.v1

Keywords: neutrinos; effective field theory; beyond standard model

Article

Unveiling New Physics Models through meson decays and their impact on neutrino experiments

Adriano Cherchiglia

Instituto de Física Gleb Wataghin - UNICAMP, 13083-859, Campinas SP, Brazil; alche@unicamp.br

Abstract: As neutrino experiments enter into the precision era, it is desirable to identify deviations from data in comparison to theory as well as provide possible models as explanation. Particularly useful is the description in terms of non-standard interactions (NSI), which can be related to neutral (NC-NSI) or charged (CC-NSI) currents. Previously, we have developed the code `eft-neutrino` that connects NSI with generic UV models at tree-level matching. In this work, we integrate our code with other tools, increasing the matching between the UV and IR theories to one-loop level. As working example, we consider the pion and kaon decay, the main production mechanisms for accelerator neutrino experiments. We provide up-to-date allowed regions on a set of Wilson coefficients related to pion and kaon decay. We also illustrate how our chain of codes can be used in particular UV models, showing that promising large value for CC-NSI can be misleading when considering a specific UV model.

Keywords: neutrinos; effective field theory; beyond standard model

---

1. Introduction

Neutrino physics is approaching the precision era, given the development of a new generation of accelerator, atmospheric and astrophysical facilities. The Deep Underground Neutrino Experiment (DUNE) are now under construction and projected to deliver sub-percent measurements of oscillation parameters and lepton–universality tests [1,2]. In Japan, Hyper-Kamiokande will bring an eight-fold mass increase over Super-K and will start data-taking in 2027, providing complementary sensitivity to proton decay, supernova neutrinos and CP violation in the lepton sector [3]. At the energy frontier, forward detectors such as FASERν and SND@LHC have already observed the first TeV-scale neutrino interactions and aim to measure $\mathcal{O}(10^4)$ charged–current (CC) events by the end of LHC Run-3, opening a qualitatively new window on neutrino interactions and forward meson production [4,5].

All of these beamlines depend overwhelmingly on leptonic meson decays for their fluxes. The channels $\pi^\pm \to \mu^\pm \nu_\mu$ and $K^\pm \to \mu^\pm \nu_\mu$ alone supply more than 90% of the ν_μ flux at DUNE and Hyper-K, while forward π/K decays generate the bulk of the LHC neutrino spectrum. Thanks to experimental control of decay rates and lattice-QCD calculations of hadronic matrix elements, these processes are among the cleanest electroweak observables; The latest NA62 branching-ratio measurement [6], when interpreted within the low-energy–effective–theory (LEFT) framework, already forces the dominant vector-type $\Delta S = 1$ coefficient to satisfy $\mathcal{O}(10^{-4})$ TeV^{-2} as shown by EFT analyses in Refs. [7,8]. Comparable—or even stronger—bounds apply to scalar and tensor structures [9]. Given such precision, any deviation seen by upcoming neutrino detectors could plausibly originate in the *production* stage and would point to charged non-standard interactions (CC-NSI) or other beyond-the-Standard-Model (BSM) effects in meson decay.

Non-standard neutrino interactions were first introduced by Wolfenstein in 1978 to describe coherent forward scattering in matter [10]. Comprehensive reviews by Ohlsson [11] and by Farzan & Tortola [12] summarise three decades of phenomenology, while more recent global fits highlight the parameter degeneracies that next-generation beams must resolve [13]. Model builders have explored many ultraviolet (UV) origins, including scalar doublets, vector leptoquarks and $U(1)'$ gauge

doi:10.20944/preprints202505.1067.v1

bosons; several of these scenarios generate sizeable CC-NSI only at the one-loop level, thereby evading tree-level constraints, see for instance [14–25].

The natural language to connect such UV completions with experimental observables is Effective Field Theory (EFT). Below the electroweak scale, the LEFT describes meson decays through five four-fermion operators whose Wilson coefficients are denoted $\epsilon_{L,R,S,P,T}$. These coefficients match onto the Standard-Model EFT (SMEFT) at $v \simeq 246\,\text{GeV}$ and can then be evolved up to any heavy mass scale. The complete tree-level LEFT↔SMEFT dictionary was completed in [26], while the one-loop extension was presented in [27]. Loop effects are crucial. For instance, they can enforce correlations with flavour-changing processes that would be invisible in a purely low-energy fit.

A set of public codes now renders this multi-scale programme computationally possible. Among those, `flavio` provides predictions and likelihoods for hundreds of flavour observables [28]; `wilson` performs renormalisation-group running and threshold matching across SMEFT, LEFT and QED/QCD EFTs [29]; while `smelli` wraps these ingredients into a global likelihood engine [30]. From a top-down perspective, codes such as `matchmakereft` [31] and `Matchete` [32] aim to provide the one-loop matching from given UV models to the SMEFT or LEFT. Focusing exclusively on the SMEFT as target EFT, `SOLD` [33,34] is particularly useful. It not only provides a user-friendly implementation of tree-level matching results presented in [35], but also extends those to one-loop matching (restricted at present to UV models containing fermions or scalars). Focusing on neutrinos experiments, in [36] we have developed the code `eft-neutrinos`, which provides the UV connection to Wilson coefficients in the LEFT automatically, at tree-level matching.

In this work, we extend our previous analysis to one-loop matching, relying on the recent developments of `SOLD`. In particular, we aim to map the models that could be behind possible anomalies detected in future neutrino experiments such as DUNE, HyperK, and Faserν. For pion decay, we have already mapped all the UV realizations at tree-level matching in a previous work [36]. We will go beyond these findings by extending the matching to one-loop order. We will also generalize the results to include kaon decay.

This work is organized as follows: in section 2 we present the methodology employed in our work, as well as setting the notation used. In section 3 we present our results, in particular the bounds on the CC-NSI as well as in the SMEFT WC relevant for pion and kaon decay. In section 4 we put our findings into perspective and conclude.

2. Methodology

Given the non-observation of unexpected resonances at the LHC, the influence of new heavy states can only be detected indirectly. This task is generally accomplished by resorting to an effective field theory approach, where the impact of BSM states is encapsulated into Wilson coefficients. In order to access the present constraints on dimension-six SMEFT WCs, we employed the codes `flavio`, `wilson`, and `smelli` [28–30]. The connection to UV models can be achieved with the help of `SOLD` [33,34]. The chain of codes employed can be summarized in figure 1. Here, we used `eft-neutrinos` [36] to obtain the WCs of SMEFT relevant for pion and kaon decay. Then, we used `flavio`, `wilson`, and `smelli` to obtain the present bounds on those WCs. After, we used `SOLD` to find the UV models at one-loop matching that could also generate those WCs. We have chosen one of such UV models, finding all the WCs that they could generate, apart from the ones connected directly to pion and kaon decay. Equipped with this knowledge, we reprocessed the results in `flavio`, `wilson`, and `smelli`, which finally gave the ultimate allowed values for the CC-NSI.

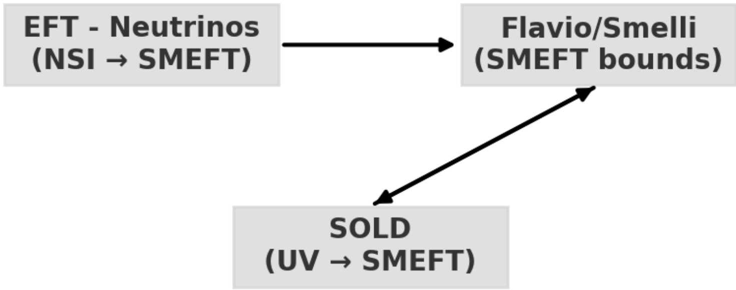

Figure 1. Chain of codes employed in our analysis.

In the next section we present the UV models relevant for meson decay, as well as the current constraints on SMEFT WCs related to these observables. In the remaining of the section we briefly discuss our notation.

In neutrino accelerator experiments, neutrinos are mainly produced by charged-current processes. In this case, it is natural to employ an EFT where the $W^{\pm}$, Z bosons were integrated, which we denote by WEFT. The Wilson Coefficients for the WEFT are commonly denoted Non-Standard Interactions (NSI). For our purposes, the relevant part of the EFT Lagrangian is given by [26,37]

$$\begin{aligned}\mathcal{L}_{\rm WEFT} \supset -\frac{2\,V_{jk}}{v^2}\Big\{ &[1+\epsilon_L^{jk}]_{\alpha\beta}\left(\bar{u}^j\gamma^\mu P_L d^k\right)\left(\bar{\ell}_\alpha\gamma_\mu P_L\nu_\beta\right) + [\epsilon_R^{jk}]_{\alpha\beta}\left(\bar{u}^j\gamma^\mu P_R d^k\right)\left(\bar{\ell}_\alpha\gamma_\mu P_L\nu_\beta\right)\\ &+\frac{1}{2}\left[\epsilon_S^{jk}\right]_{\alpha\beta}\left(\bar{u}^j d^k\right)\left(\bar{\ell}_\alpha P_L\nu_\beta\right) - \frac{1}{2}\left[\epsilon_P^{jk}\right]_{\alpha\beta}\left(\bar{u}^j\gamma^5 d^k\right)\left(\bar{\ell}_\alpha P_L\nu_\beta\right)\\ &+\frac{1}{4}\left[\epsilon_T^{jk}\right]_{\alpha\beta}\left(\bar{u}^j\sigma^{\mu\nu}P_L d^k\right)\left(\bar{\ell}_\alpha\sigma_{\mu\nu}P_L\nu_\beta\right) + \text{h.c.}\Big\}\,, \end{aligned} \tag{1}$$

We assume that all charged fermions are in the mass eigenstate basis, V is the CKM matrix, and $v \approx 246$ GeV is the Higgs vacuum expectation value. We can relate this Lagrangian to more commonly used Low Energy EFT (LEFT) Lagrangian, which renders the following connection in the notation of [26]

$$L_r^{V,LL} = -\frac{2\,V_{kj}^*}{v^2}\left[\delta_{\beta\alpha} + (\epsilon_L^{kj})_{\beta\alpha}\right]^*, \qquad L_r^{V,LR} = -\frac{2\,V_{kj}^*}{v^2}(\epsilon_R^{kj})^*_{\beta\alpha}, \tag{2}$$

$$L_r^{S,RR} + L_r^{S,RL} = -\frac{2V_{kj}^*}{v^2}(\epsilon_S^{kj})^*_{\beta\alpha}, \qquad L_r^{S,RL} - L_r^{S,RR} = -\frac{2V_{kj}^*}{v^2}(\epsilon_P^{kj})^*_{\beta\alpha}, \tag{3}$$

$$L_r^{T,RR} = -\frac{V_{kj}^*}{2v^2}(\epsilon_T^{kj})^*_{\beta\alpha}, \tag{4}$$

where $r = {}^{\nu edu}_{\alpha\beta jk}$ and we are using an asterisk to denote complex conjugation here. One can perform the matching to the SMEFT, which was done in [26]. For completeness, we reproduce it below

$$L^{V,LL}_{\substack{\nu edu\\ prst}} = \sum_x V_{xs}^* L^{V,LL}_{\substack{\nu edu\\ prxt}} = \sum_x V_{xs}^*\left(2C^{(3)}_{\substack{lq\\ prxt}} - \frac{\bar{g}_2{}^2}{2M_W^2}[W_l]_{pr}[W_q]^*_{tx}\right), \tag{5}$$

$$L^{V,LR}_{\substack{\nu edu\\ prst}} = -\frac{\bar{g}_2{}^2}{2M_W^2}[W_l]_{pr}[W_R]^*_{ts}, \tag{6}$$

$$L^{S,RR}_{\substack{\nu edu\\ prst}} = \sum_x V_{xs}^* C^{(1)}_{\substack{lequ\\ prxt}}, \quad L^{S,RL}_{\substack{\nu edu\\ prst}} = C_{\substack{ledq\\ prst}}, \quad L^{T,RR}_{\substack{\nu edu\\ prst}} = \sum_x V_{xs}^* C^{(3)}_{\substack{lequ\\ prxt}}, \tag{7}$$

where

$$[W_l]_{pr} = \left[\delta_{pr} + v_T^2 C^{(3)}_{\substack{Hl\\ pr}}\right], \quad [W_q]_{pr} = \left[\delta_{pr} + v_T^2 C^{(3)}_{\substack{Hq\\ pr}}\right], \quad [W_R]_{pr} = \left[\frac{1}{2}v_T^2 C_{\substack{Hud\\ pr}}\right]. \tag{8}$$

 doi:10.20944/preprints202505.1067.v1

We are adopting the so-called up basis where the up quark and charged lepton Yukawa matrices are diagonal.

In order to connect the CC-NSI to neutrino experiments, we employ a quantum field theory (QFT) framework [38–41]. For accelerator neutrino experiments, where neutrinos are produced trough pion decay, we obtain that the differential event rate for neutrinos produced with flavor α to be detected with flavor β and energy E_ν at a detector distant L from the source S is given by [42]

$$R^S_{\alpha\beta} = N_T \sigma^{\rm SM}_\beta(E_\nu) \Phi^{\rm SM}_\alpha(E_\nu) \sum_{k,l} e^{-i\frac{L\Delta m^2_{kl}}{2E_\nu}} \frac{[\mathcal{P}U]_{\alpha l}[U^\dagger \mathcal{P}^\dagger]_{k\alpha}}{[\mathcal{P}\mathcal{P}^\dagger]_{\alpha\alpha}} U_{\beta k} U^*_{\beta l}\,, \tag{9}$$

where $\Phi^{\rm SM}_\alpha$ is the SM flux, while $\sigma^{\rm SM}_\beta$ is the SM cross-section. The matrix U_{ij} is the PMNS matrix, while the matrix $\mathcal{P}$ is given by

$$[\mathcal{P}]_{\alpha\beta} \equiv \delta_{\alpha\sigma} + \bar\epsilon_{\alpha\sigma}, \quad \text{where} \quad \bar\epsilon_{\alpha\sigma} = (\epsilon_L)_{\alpha\sigma} - (\epsilon_R)_{\alpha\sigma} - \frac{m^2_{\pi^\pm}}{m_{\ell_\alpha}(m_u + m_d)}(\epsilon_P)_{\alpha\sigma}\,. \tag{10}$$

It is clear from the equation above that neutrino accelerator experiments are sensitive only to the direction $\bar\epsilon_{\alpha\sigma}$. It is straightforward to express the CC-NSI parameters in terms of the WC of the SMEFT, which we also reproduce below for completeness [36]

$$\bar\epsilon_{\beta\alpha} = \frac{v^2}{2}\left[2C^{(3)}_{\substack{Hl\\ \alpha\beta}} + 2\sum_x V^*_{x1}\left(\delta_{\alpha\beta} C^{(3)*}_{\substack{Hq\\ 1x}} - C^{(3)}_{\substack{lq\\ \alpha\beta 1x}}\right) + \delta_{\alpha\beta} C^*_{\substack{Hud\\ 11}} + p_\beta\left(C_{\substack{ledq\\ \alpha\beta 11}} - \sum_x V^*_{x1} C^{(1)}_{\substack{lequ\\ \alpha\beta x1}}\right)\right]^*. \tag{11}$$

where we used the notation $p_\alpha = \frac{m^2_{\pi^\pm}}{m_{\ell_\alpha}(m_u+m_d)}$.

3. Results

Given the chain introduced in figure 1 we have obtained the present constrains on all SMEFT WCs relevant to pion and kaon decay. The results can be seen in Figures 2–4.

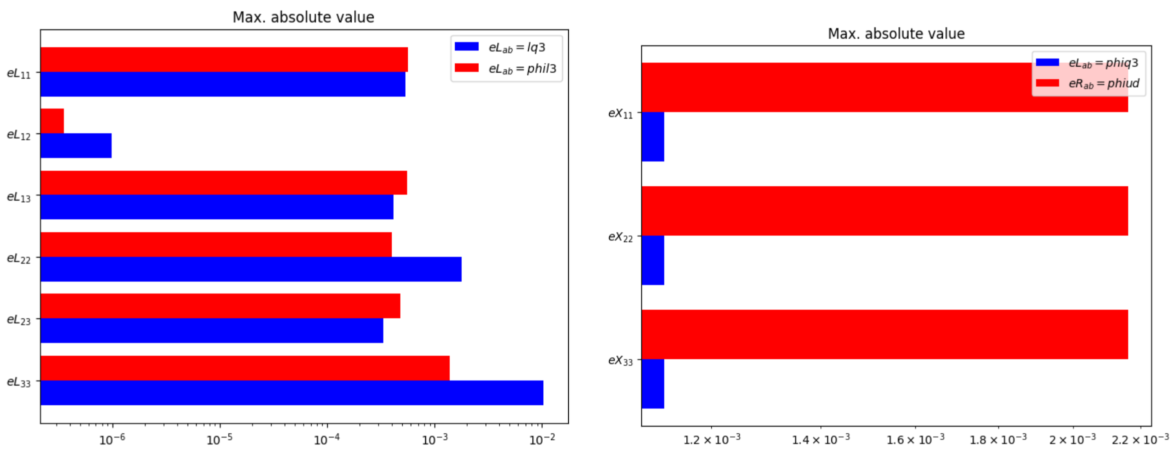

(a) (b)

Figure 2. *Cont.*

 doi:10.20944/preprints202505.1067.v1

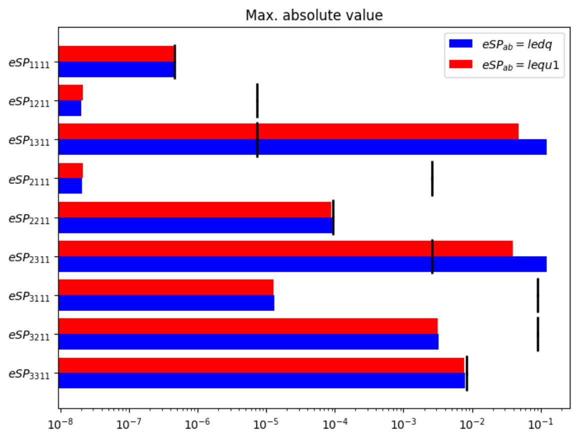

(**c**)

Figure 2. Bounds on the CC-NSI $\epsilon_{L,R,P}$ that affect pion decay: (**a**) Bound on ϵ_L due to SMEFT WCs $C^{(3)}_{Hl}$, and $C^{(3)}_{lq}$. (**b**) Bound on ϵ_L due to SMEFT WC $C^{(3)}_{Hq}$, and on ϵ_R due to $C^{(3)}_{Hud}$. (**c**) Bound on ϵ_P due to SMEFT WCs C_{ledq}, and $C^{(1)}_{lequ}$. In black we depict the bounds coming directly from pion or tau decay [43].

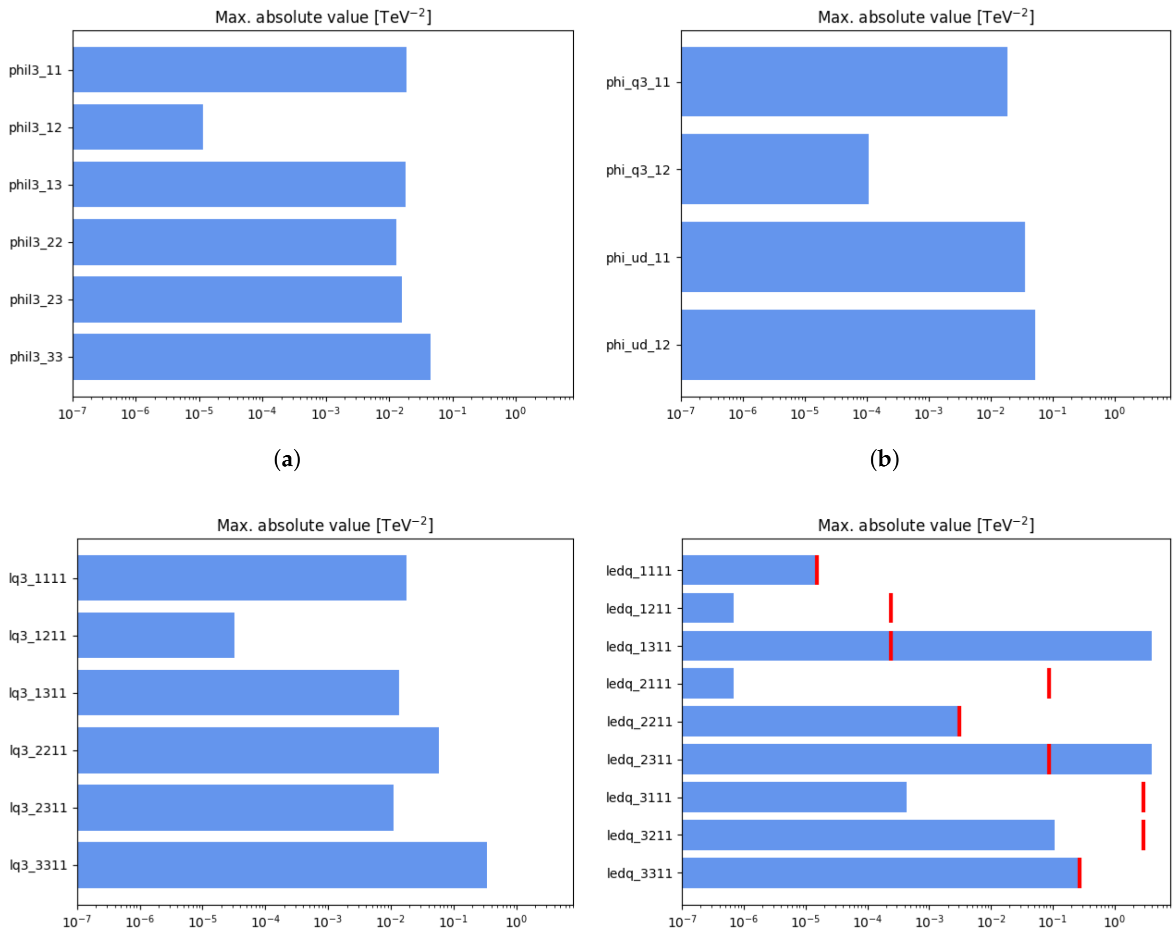

(**a**) (**b**) (**c**) (**d**)

Figure 3. *Cont.*

Preprints.org (www.preprints.org) | NOT PEER-REVIEWED | Posted: 14 May 2025 doi:10.20944/preprints202505.1067.v1

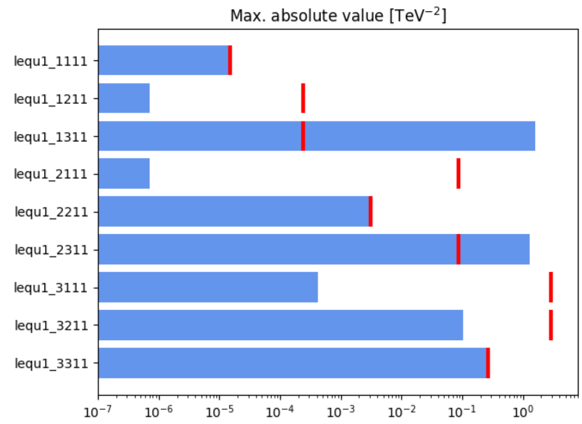

(**e**)

Figure 3. Bounds on the SMEFT WC that affect pion decay: (**a**) Bound on $C_{Hl}^{(3)}$. (**b**) Bounds on $C_{Hq}^{(3)}$, and $C_{Hud}^{(3)}$. Notice that indices 11 (12) are relevant for pion(kaon) decay. (**c**) Bound on $C_{lq}^{(3)}$. (**d**) Bound on C_{ledq}. In red we depict the bounds coming directly from pion or tau decay [43]. (**e**) Bound on $C_{lequ}^{(1)}$. In red we depict the bounds coming directly from pion or tau decay [43].

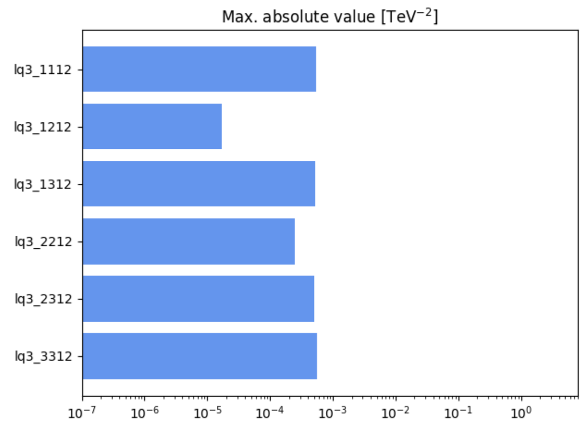

(**a**)

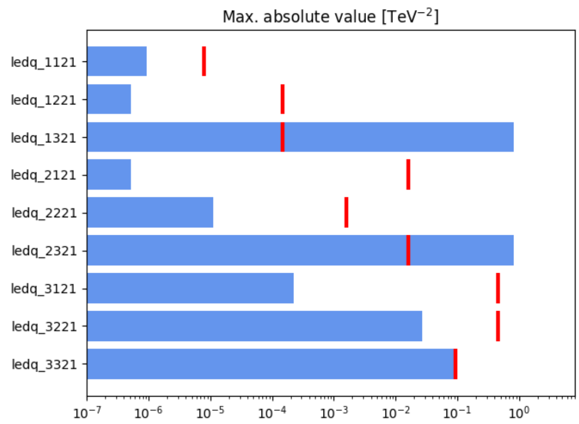

(**b**)

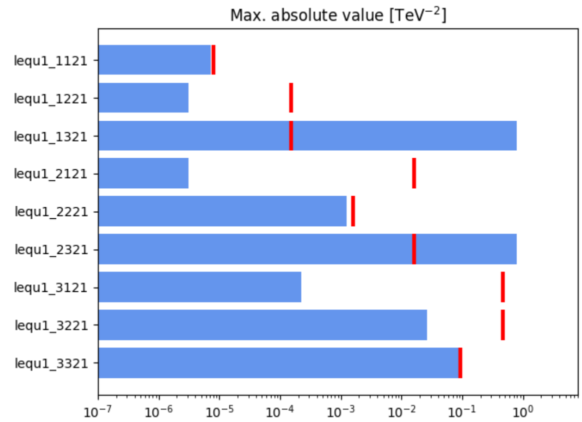

(**c**)

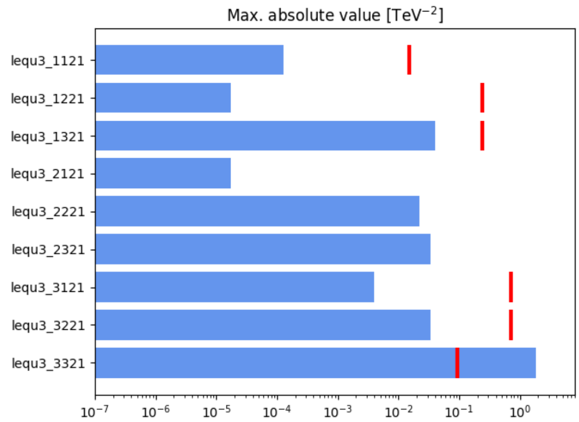

(**d**)

Figure 4. Bounds on the SMEFT WC that affect kaon decay: (**a**) Bound on $C_{lq}^{(3)}$. (**b**) Bound on C_{ledq}. In red we depict the bounds coming directly from kaon or tau decay [43]. (**c**) Bound on $C_{lequ}^{(1)}$. In red we depict the bounds coming directly from kaon or tau decay [43]. (**d**) Bound on $C_{lequ}^{(3)}$. In red we depict the bounds coming directly from kaon or tau decay [43].

Preprints.org (www.preprints.org) | NOT PEER-REVIEWED | Posted: 14 May 2025 doi:10.20944/preprints202505.1067.v1

In figure 2 we show the bounds on CC-NSI relevant for pion decay, namely $\epsilon_{L,R,P}$. By considering only one SMEFT WC non-null at time, we obtain the red/blue bands. We also include as black lines the current limits extracted directly from pion or tau decay experiments [43]. In figure 3 we show the bounds on each SMEFT WC that enter in the prediction of the pion decay rate. We consider only one non-null WC at time. In red we show the present limits coming directly from pion or tau decay [43]. A similar figure can be devised for the SMEFT WC that impact the kaon decay. We show the present bounds on figure 4, where in red we represent the direct limits from kaon or tau decay [43].

Regarding the SMEFT WCs related to pion decay, as the plots clear show, the WCs $C_{\substack{ledq\\1311}}$, $C_{\substack{ledq\\2311}}$, $C^{(1)}_{\substack{lequ\\1311}}$, $C^{(1)}_{\substack{lequ\\2311}}$ are the least constrained by *flavio*. However, one needs to add the bound that comes directly from pion decay, which reduces significantly the maximum allowed value for $C_{\substack{ledq\\1311}}$, $C^{(1)}_{\substack{lequ\\1311}}$. Therefore, we will seek models that can generate $C_{\substack{ledq\\2311}}$, $C^{(1)}_{\substack{lequ\\2311}}$.

The complete list of UV models up to one-loop matching relevant to pion and kaon decay is provided into the repository `eft-neutrinos`[1]. As illustrative example we consider an UV model containing a leptoquark ω_1. Its quantum numbers under the $SU(3) \times SU(2) \times U(1)$ gauge group are $(3, 1, -\frac{1}{3})$. Performing the one-loop matching with `SOLD` we obtain

$$C_{\substack{ledq\\ij11}} = \sum_{x,y=1}^{3} \frac{y^{eu}_{jx}\, \bar{y}^{du}_{1x}\, y^{qq}_{y1}\, \bar{y}^{ql}_{iy}}{4\pi^2 M^2_{\omega_1}} \tag{12}$$

This model generates other WC at one-loop matching, such as $C^{(1)}_{\substack{lequ\\ij11}}$. Actually, there is a contribution already at tree-level. In order to suppress those, we will consider couplings with third generation quarks in the loop. In other words, we only consider the case $x = y = 3$. Under this scenario, the one-loop matching to $C^{(1)}_{\substack{lequ\\ij11}}$ is null. Therefore, we will consider a UV model containing ω_1 where only the couplings y^{eu}_{33}, y^{du}_{13}, y^{qq}_{31}, y^{ql}_{23}, are non-null. We also consider that they are real for simplicity. Under these circumstances, we found the allowed region on those parameters. The result can be seen in Figure 5

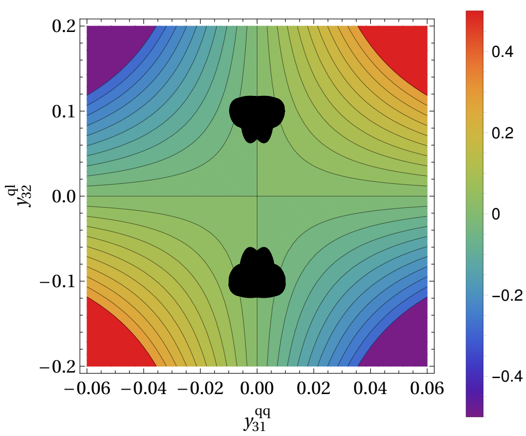

Figure 5. Allowed region on y^{qq}_{31}, y^{ql}_{23} at 90% C.L. in black. Contour lines (in units of 10^{-3}) for different values of $C_{\substack{ledq\\2311}}$, considering $y^{eu}_{33} = 1$, $y^{du}_{13} = 1$, and $M_{\omega_1} = 600$ GeV.

In Figure 5 we show in black the 90% C.L. allowed region on the parameters y^{qq}_{31}, y^{ql}_{23}. We are considering $y^{eu}_{33} = 1$, $y^{du}_{13} = 1$, and $M_{\omega_1} = 600$ GeV. Using those values, we can also find the contours

[1] https://gitlab.com/alcherchiglia/eft-neutrinos

for different values of $C_{\substack{ledq\\2311}}$, which we also display. The values should be multiplied by 10^{-3}. After imposing bounds coming from other WCs, we find that $C_{\substack{ledq\\2311}}$ can be at most 10^{-4} TeV^{-2}. Therefore, the allowed CC-NSI ϵ_P in this UV model is much lower than our initial analysis suggested. A similar reasoning can be applied to WC $C_{\substack{ledq\\2321}}$ that affects kaon decay. We have checked that same the pattern depicted in figure 5 emerges, where the only difference is that y^{du}_{23} is non-null (and equal to one).

Other interesting UV model is the one where we add a scalar doublet φ, whose quantum numbers are $(1, 2, \frac{1}{2})$. We assume no-mixing with the standard higgs doublet, and that φ does not develop a vev. Also, only a specific combination of Yukawas are non-null, namely y^d_{11} and y^e_{23}. Therefore, already at tree-level matching there is a contribution

$$C_{\substack{ledq\\ij11}} = \frac{\bar{y}^e_{ji}\, y^d_{11}}{M^2_\varphi} \tag{13}$$

We have performed the one-loop matching to the SMEFT of this model under the assumption that only y^d_{11} and y^e_{23} are non-null. As expected, many other operators are induced. However, the stronger bounds still come from pion decay, setting

$$C_{\substack{ledq\\2311}} < 8 \times 10^{-2} \tag{14}$$

Thus, for order one couplings, the lower bound on the scalar mass is of order 3.5 TeV.

For the case of $C_{\substack{ledq\\2321}}$, that enters in the kaon decay prediction, we need only to consider y^d_{21} non-null instead of y^d_{11}. We have performed this analysis, and checked that the strongest bound is still coming from kaon decay directly, namely

$$C_{\substack{ledq\\2321}} < 1.7 \times 10^{-2} \tag{15}$$

Thus, for order one couplings, the lower bound on the scalar mass is of order 7.6 TeV.

Another models can be devised as well, using the results in the repository `eft-neutrinos`. A thorough investigation is beyond the scope of this work, since our main aim was to provide and exemplify the chain of codes depicted in Figure 1.

4. Discussion

Neutrino experiments are delving into the precision era. In this scenario, the constrains on new phenomena will either become tidier or a clean sign of new physics will emerge. In order to help navigate into the latter case, the usage of effective field theories is particularly promising. This approach provides a consistent way to connect low-energy phenomena (extracted at neutrino experiments, for instance) with the possible underlying UV models.

In this work we have focused on possible new phenomena perceived in accelerator neutrino experiments, from modifications at the standard pion or kaon decay. The imprints of such new phenomena can be conveniently written as CC-NSI. Using an EFT approach, we mapped all models with BSM fermions or scalars at one-loop matching that could affect the pion or kaon decay rate. Once a model was chosen, we illustrated how bounds from other sources (mainly flavor experiments) could play a role on constraining the maximum allowed CC-NSI.

Funding: A.C. acknowledges support from National Council for Scientific and Technological Development—CNPq.

Data Availability Statement: Data used in this work can be found in the repository `eft-neutrinos`[2].

[2] https://gitlab.com/alcherchiglia/eft-neutrinos

 doi:10.20944/preprints202505.1067.v1

Conflicts of Interest: The author declare no conflicts of interest. The funders had no role in the design of the study; in the collection, analyses, or interpretation of data; in the writing of the manuscript; or in the decision to publish the results.

Abbreviations

The following abbreviations are used in this manuscript:

UV	Ultra-violet
IR	Infrared
WC	Wilson coefficient
BSM	Beyond Standard Model
EFT	Effective Field Theory
NC-NSI	Neutral non-standard interactions
CC-NSI	Charged non-standard interactions

References

1. Abi, B.; et al. Deep Underground Neutrino Experiment (DUNE), Far Detector Technical Design Report, Volume II: DUNE Physics **2020**. [arXiv:hep-ex/2002.03005].
2. Abi, B.; et al. Prospects for beyond the Standard Model physics searches at the Deep Underground Neutrino Experiment. *Eur. Phys. J. C* **2021**, *81*, 322, [arXiv:hep-ex/2008.12769]. https://doi.org/10.1140/epjc/s10052-021-09007-w.
3. Abe, K.; et al. Hyper-Kamiokande Design Report **2018**. [arXiv:physics.ins-det/1805.04163].
4. Mammen Abraham, R.; et al. First Measurement of νe and $\nu\mu$ Interaction Cross Sections at the LHC with FASER's Emulsion Detector. *Phys. Rev. Lett.* **2024**, *133*, 021802, [arXiv:hep-ex/2403.12520]. https://doi.org/10.1103/PhysRevLett.133.021802.
5. Abreu, H.; et al. First Direct Observation of Collider Neutrinos with FASER at the LHC. *Phys. Rev. Lett.* **2023**, *131*, 031801, [arXiv:hep-ex/2303.14185]. https://doi.org/10.1103/PhysRevLett.131.031801.
6. Cortina Gil, E.; et al. Measurement of the very rare $K^+ \to \pi^+ \nu\bar{\nu}$ decay. *JHEP* **2021**, *06*, 093, [arXiv:hep-ex/2103.15389]. https://doi.org/10.1007/JHEP06(2021)093.
7. Li, T.; Ma, X.D.; Schmidt, M.A. Implication of $K \to \pi\nu\bar{\nu}$ for generic neutrino interactions in effective field theories. *Phys. Rev. D* **2020**, *101*, 055019, [arXiv:hep-ph/1912.10433]. https://doi.org/10.1103/PhysRevD.101.055019.
8. Gorbahn, M.; Moldanazarova, U.; Sieja, K.H.; Stamou, E.; Tabet, M. The anatomy of $K^+ \to \pi^+\nu\bar{\nu}$ distributions. *Eur. Phys. J. C* **2024**, *84*, 680, [arXiv:hep-ph/2312.06494]. https://doi.org/10.1140/epjc/s10052-024-13027-7.
9. Deppisch, F.F.; Fridell, K.; Harz, J. Constraining lepton number violating interactions in rare kaon decays. *JHEP* **2020**, *12*, 186, [arXiv:hep-ph/2009.04494]. https://doi.org/10.1007/JHEP12(2020)186.
10. Wolfenstein, L. Neutrino Oscillations in Matter. *Phys. Rev. D* **1978**, *17*, 2369–2374. https://doi.org/10.1103/PhysRevD.17.2369.
11. Ohlsson, T. Status of non-standard neutrino interactions. *Rept. Prog. Phys.* **2013**, *76*, 044201, [arXiv:hep-ph/1209.2710]. https://doi.org/10.1088/0034-4885/76/4/044201.
12. Farzan, Y.; Tortola, M. Neutrino oscillations and Non-Standard Interactions. *Front. in Phys.* **2018**, *6*, 10, [arXiv:hep-ph/1710.09360]. https://doi.org/10.3389/fphy.2018.00010.
13. Coloma, P.; Gonzalez-Garcia, M.C.; Maltoni, M.; Pinheiro, J.a.P.; Urrea, S. Global constraints on non-standard neutrino interactions with quarks and electrons. *JHEP* **2023**, *08*, 032, [arXiv:hep-ph/2305.07698]. https://doi.org/10.1007/JHEP08(2023)032.
14. Bergmann, S.; Grossman, Y.; Pierce, D.M. Can lepton flavor violating interactions explain the atmospheric neutrino problem? *Phys. Rev. D* **2000**, *61*, 053005, [hep-ph/9909390]. https://doi.org/10.1103/PhysRevD.61.053005.
15. Antusch, S.; Baumann, J.P.; Fernandez-Martinez, E. Non-Standard Neutrino Interactions with Matter from Physics Beyond the Standard Model. *Nucl. Phys. B* **2009**, *810*, 369–388, [arXiv:hep-ph/0807.1003]. https://doi.org/10.1016/j.nuclphysb.2008.11.018.
16. Gavela, M.B.; Hernandez, D.; Ota, T.; Winter, W. Large gauge invariant non-standard neutrino interactions. *Phys. Rev. D* **2009**, *79*, 013007, [arXiv:hep-ph/0809.3451]. https://doi.org/10.1103/PhysRevD.79.013007.

17. Meloni, D.; Ohlsson, T.; Winter, W.; Zhang, H. Non-standard interactions versus non-unitary lepton flavor mixing at a neutrino factory. *JHEP* **2010**, *04*, 041, [arXiv:hep-ph/0912.2735]. https://doi.org/10.1007/JHEP04(2010)041.
18. Altmannshofer, W.; Tammaro, M.; Zupan, J. Non-standard neutrino interactions and low energy experiments. *JHEP* **2019**, *09*, 083, [arXiv:hep-ph/1812.02778]. [Erratum: JHEP 11, 113 (2021)], https://doi.org/10.1007/JHEP11(2021)113.
19. Babu, K.S.; Dev, P.S.B.; Jana, S.; Thapa, A. Non-Standard Interactions in Radiative Neutrino Mass Models. *JHEP* **2020**, *03*, 006, [arXiv:hep-ph/1907.09498]. https://doi.org/10.1007/JHEP03(2020)006.
20. Bischer, I.; Rodejohann, W. General neutrino interactions from an effective field theory perspective. *Nucl. Phys. B* **2019**, *947*, 114746, [arXiv:hep-ph/1905.08699]. https://doi.org/10.1016/j.nuclphysb.2019.114746.
21. Davidson, S.; Gorbahn, M. Charged lepton flavor change and nonstandard neutrino interactions. *Phys. Rev. D* **2020**, *101*, 015010, [arXiv:hep-ph/1909.07406]. https://doi.org/10.1103/PhysRevD.101.015010.
22. Terol-Calvo, J.; Tórtola, M.; Vicente, A. High-energy constraints from low-energy neutrino nonstandard interactions. *Phys. Rev. D* **2020**, *101*, 095010, [arXiv:hep-ph/1912.09131]. https://doi.org/10.1103/PhysRevD.101.095010.
23. Babu, K.S.; Gonçalves, D.; Jana, S.; Machado, P.A.N. Neutrino Non-Standard Interactions: Complementarity Between LHC and Oscillation Experiments. *Phys. Lett. B* **2021**, *815*, 136131, [arXiv:hep-ph/2003.03383]. https://doi.org/10.1016/j.physletb.2021.136131.
24. Du, Y.; Li, H.L.; Tang, J.; Vihonen, S.; Yu, J.H. Non-standard interactions in SMEFT confronted with terrestrial neutrino experiments. *JHEP* **2021**, *03*, 019, [arXiv:hep-ph/2011.14292]. https://doi.org/10.1007/JHEP03(2021)019.
25. Du, Y.; Li, H.L.; Tang, J.; Vihonen, S.; Yu, J.H. Exploring SMEFT induced nonstandard interactions: From COHERENT to neutrino oscillations. *Phys. Rev. D* **2022**, *105*, 075022, [arXiv:hep-ph/2106.15800]. https://doi.org/10.1103/PhysRevD.105.075022.
26. Jenkins, E.E.; Manohar, A.V.; Stoffer, P. Low-Energy Effective Field Theory below the Electroweak Scale: Operators and Matching. *JHEP* **2018**, *03*, 016, [arXiv:hep-ph/1709.04486]. [Erratum: JHEP 12, 043 (2023)], https://doi.org/10.1007/JHEP03(2018)016.
27. Dekens, W.; Stoffer, P. Low-energy effective field theory below the electroweak scale: matching at one loop. *JHEP* **2019**, *10*, 197, [arXiv:hep-ph/1908.05295]. [Erratum: JHEP 11, 148 (2022)], https://doi.org/10.1007/JHEP10(2019)197.
28. Straub, D.M. flavio: A Python package for flavour and precision phenomenology in the Standard Model and beyond **2018**. [arXiv:hep-ph/1810.08132].
29. Aebischer, J.; Kumar, J.; Straub, D.M. Wilson: A Python package for the running and matching of Wilson coefficients above and below the electroweak scale. *Eur. Phys. J. C* **2018**, *78*, 1026, [arXiv:hep-ph/1804.05033]. https://doi.org/10.1140/epjc/s10052-018-6492-7.
30. Aebischer, J.; Kumar, J.; Stangl, P.; Straub, D.M. A Global Likelihood for Precision Constraints and Flavour Anomalies. *Eur. Phys. J. C* **2019**, *79*, 509, [arXiv:hep-ph/1810.07698]. https://doi.org/10.1140/epjc/s10052-019-6977-z.
31. Carmona, A.; Lazopoulos, A.; Olgoso, P.; Santiago, J. Matchmakereft: Automated tree-level and one-loop matching. *SciPost Phys.* **2022**, *12*, 198, [arXiv:hep-ph/2112.10787]. https://doi.org/10.21468/SciPostPhys.12.6.198.
32. Fuentes-Martín, J.; König, M.; Pagès, J.; Thomsen, A.E.; Wilsch, F. A proof of concept for matchete: An automated tool for matching effective theories. *Eur. Phys. J. C* **2023**, *83*, 662, [arXiv:hep-ph/2212.04510]. https://doi.org/10.1140/epjc/s10052-023-11726-1.
33. Guedes, G.; Olgoso, P.; Santiago, J. Towards the one loop IR/UV dictionary in the SMEFT: One loop generated operators from new scalars and fermions. *SciPost Phys.* **2023**, *15*, 143, [arXiv:hep-ph/2303.16965]. https://doi.org/10.21468/SciPostPhys.15.4.143.
34. Guedes, G.; Olgoso, P. From the EFT to the UV: The complete SMEFT one-loop dictionary **2024**. [arXiv:hep-ph/2412.14253].
35. de Blas, J.; Criado, J.C.; Perez-Victoria, M.; Santiago, J. Effective description of general extensions of the Standard Model: the complete tree-level dictionary. *JHEP* **2018**, *03*, 109, [arXiv:hep-ph/1711.10391]. https://doi.org/10.1007/JHEP03(2018)109.
36. Cherchiglia, A.; Santiago, J. DUNE potential as a new physics probe. *JHEP* **2024**, *03*, 018, [arXiv:hep-ph/2309.15924]. https://doi.org/10.1007/JHEP03(2024)018.

37. Cirigliano, V.; Jenkins, J.; Gonzalez-Alonso, M. Semileptonic decays of light quarks beyond the Standard Model. *Nucl. Phys. B* **2010**, *830*, 95–115, [arXiv:hep-ph/0908.1754]. https://doi.org/10.1016/j.nuclphysb.2009.12.020.
38. Giunti, C.; Kim, C.W.; Lee, J.A.; Lee, U.W. On the treatment of neutrino oscillations without resort to weak eigenstates. *Phys. Rev. D* **1993**, *48*, 4310–4317, [hep-ph/9305276]. https://doi.org/10.1103/PhysRevD.48.4310.
39. Akhmedov, E.K.; Kopp, J. Neutrino Oscillations: Quantum Mechanics vs. Quantum Field Theory. *JHEP* **2010**, *04*, 008, [arXiv:hep-ph/1001.4815]. [Erratum: JHEP 10, 052 (2013)], https://doi.org/10.1007/JHEP04(2010)008.
40. Kobach, A.; Manohar, A.V.; McGreevy, J. Neutrino Oscillation Measurements Computed in Quantum Field Theory. *Phys. Lett. B* **2018**, *783*, 59–75, [arXiv:hep-ph/1711.07491]. https://doi.org/10.1016/j.physletb.2018.06.021.
41. Falkowski, A.; González-Alonso, M.; Tabrizi, Z. Consistent QFT description of non-standard neutrino interactions. *JHEP* **2020**, *11*, 048, [arXiv:hep-ph/1910.02971]. https://doi.org/10.1007/JHEP11(2020)048.
42. Bresó-Pla, V.; Falkowski, A.; González-Alonso, M.; Monsálvez-Pozo, K. EFT analysis of New Physics at COHERENT. *JHEP* **2023**, *05*, 074, [arXiv:hep-ph/2301.07036]. https://doi.org/10.1007/JHEP05(2023)074.
43. Falkowski, A.; González-Alonso, M.; Kopp, J.; Soreq, Y.; Tabrizi, Z. EFT at FASERν. *JHEP* **2021**, *10*, 086, [arXiv:hep-ph/2105.12136]. https://doi.org/10.1007/JHEP10(2021)086.